Coherent control of quantum tunneling in different driving-frequency regions

Gengbiao Lu, Wenhua Hai,* Honghua Zhong, and Qiongtao Xie
Department of Physics and Key Laboratory of Low-Dimensional Quantum Structure and Quantum Control, Hunan Normal University, Ministry of Education, Changsha 410081, China

(Received 19 April 2010; published 28 June 2010)

We investigate the coherent control of quantum tunneling for a single particle held in a driven double-well potential. For a moderate-frequency region, we demonstrate that the irregular quantum tunneling is associated with classically chaotic dynamics. A set of lower resonance-like frequencies is found, for which the coherent destruction of tunneling in the sense of the time average is illustrated numerically. For a high-frequency region, it is shown that the particle is located at the bottom of each well alternately for a long time and the time located in one well can be modulated by adjusting the driving field. The results could be useful for the experiments of controlling single-particle tunneling [see, e.g., E. Kierig, U. Schnorrberger, A. Schietinger, J. Tomkovic, and M. K. Oberthaler, Phys. Rev. Lett. **100**, 190405 (2008).].

DOI: 10.1103/PhysRevA.81.063423 PACS number(s): 32.80.Qk, 03.65.Ge, 32.80.Wr, 03.75.Lm

I. INTRODUCTION

The tunneling dynamics of the periodically driven double-well system has been an attractive subject in recent years and many interesting phenomena were demonstrated, such as the coherent control of self-trapping with nonzero time average of population imbalance [1], Josephson-like oscillations [2], and photon-assisted tunneling [3]. As a relatively simple system, a single particle trapped in a double well has also been investigated widely [4–7]. Previously, Lin and Ballentine [8] proved that the tunneling rate can be highly enhanced due to the periodic modulation associated with chaos. Then Grossmann *et al.* [9] found another peculiar effect; namely, for an appropriate ratio of the driving strength and frequency, the particle initially located in one well never transfers to the other. Such an effect was called the "coherent destruction of tunneling" (CDT), which can be well understood by a two-state model in the high-frequency approximation [7]. With the development of laser shaping technology [10], the coherent control of quantum tunneling, either enhancing [8] or suppressing [9] induced by an external field, has attracted great theoretical and experimental interest. Recently, E. Kierig *et al.* [11] reported the first direct observation of coherent control for single-atom tunneling in a strongly driven double-well potential, which has exhibited the importance of studying the quantum manipulation of a single particle.

In this paper, we investigate the coherent control of quantum tunneling for a single particle which is initially static in one of the driven double wells. Three frequency regions are found based on Newton's classical equation, and the tunneling behaviors in different frequency regions are illustrated numerically. In the moderate-frequency region, the classically chaotic dynamics and the quantum irregular tunneling are demonstrated. In the low- and high-frequency regions, the classical trajectories are distributed regularly in the initially occupied well, but quantum tunneling may occur. For a given driving amplitude, quantum treatment leads to a set of resonance-like frequencies in the low-frequency region, $\omega_n = \nu/n$ with constant ν and $n = 1,2,\ldots$, which is similar to the condition of multiple photon resonance [12–14]. The spatiotemporal evolutions of probability density show that for the discrete driving frequency ω_n the particle is located completely in the initially occupied well except for n oscillations in some short time intervals. Thus, the time average of the probability density displays the approximate CDT, which is equivalent to the strong self-trapping in the sense of the time average [1]. In the high-frequency region, it is shown that the particle is located at the bottom of each well alternately for a long time and the time located in one well can be modulated by adjusting the driving field. Interestingly, the similar phenomenon of long-lasting localization in each well was observed in the recent experiment of a light coupler [15]. Based on the capacity of current experiments [11], the results presented in this paper can be tested and used experimentally.

II. QUANTUM TUNNELING AND CONTROL IN DIFFERENT FREQUENCY REGIONS

We consider a single particle held in a symmetric quartic double well and driven by a time-dependent external field. The corresponding one-dimensional Schrödinger equation reads [16]

$$i\frac{\partial}{\partial t}\Psi(x,t) = -\frac{1}{2}\frac{\partial^2}{\partial x^2}\Psi(x,t) + V(x,t)\Psi(x,t), \qquad (1)$$

where the driven double-well potential is in the form

$$V(x,t) = bx^4 - [a - \varepsilon\sin(\omega t)]\frac{x^2}{2}. \qquad (2)$$

For simplification, hereafter we adopt dimensionless parameters, where the energy is normalized in units of $\hbar\omega_0$ with ω_0 being the harmonic frequency around the deepest well [17]. The length, time, and driving frequency are in units of $\sqrt{\frac{\hbar}{m\omega_0}}$, ω_0^{-1}, and ω_0, respectively, and the constants a and ε are in units of $m\omega_0^2$ and constant b is in units of $\frac{m^2\omega_0^3}{\hbar}$.

In this model, the double-well potential is symmetric during the time-evolution process as in Fig. 1, where a few lowest eigenenergy levels in the absence of the driving field ($\varepsilon = 0$) are shown numerically. It is obvious that the potential function obeys the periodicity $V(x,t+T) = V(x,t)$ with $T = 2\pi/\omega$,

*Corresponding author: whhai2005@yahoo.com.cn

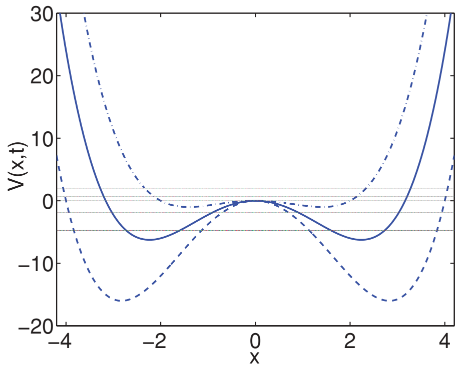

FIG. 1. (Color online) Sketch of the driven double-well potential $V(x,t)$ with $a = 5$, $b = 0.25$, and $\varepsilon = 3$ for the times $\omega t = 0$ (solid line), $\omega t = 0.5\pi$ (dash-dotted line), and $\omega t = 1.5\pi$ (dashed line). The horizontal lines denote some lower eigenenergy levels of Eq. (1) in the absence of the driving force ($\varepsilon = 0$), with the same potential parameters a and b. The lines below the barrier occur in doublets. The quantities plotted in every figure of this paper are dimensionless.

and the barrier height between wells is varied periodically with the lowest barrier at $t_k(\omega) = \frac{(2k+0.5)\pi}{\omega}$ and the deepest well at $t'_k(\omega) = \frac{(2k-0.5)\pi}{\omega}$ $(k = 0,1,2,\ldots)$.

To show the relation between quantum treatment and the corresponding classical treatment, at first we consider classical dynamics of the double-well system governed by Newton's classical equation

$$\ddot{x} - [a - \varepsilon \sin(\omega t)]x + 4bx^3 = 0. \tag{3}$$

The parameters are chosen as $a = 5$ and $b = 0.25$ throughout this paper. In addition, we set the initial position and momentum as $x_0 = \sqrt{5}$ and $p_0 = 0$, which means the particle is located at the bottom of the right well initially with zero momentum. From Eq. (3), the time evolution of the classical trajectory $x(t)$ is plotted for different driving parameters, as in Fig. 2. Given driving amplitude $\varepsilon = 3$, three frequency regions are shown as in Fig. 2(a), where the particle crosses over the barrier centered at $x = 0$ in the moderate-frequency region $\omega \in [0.5,8.9]$. But the classical crossovers do not occur in the low- and high-frequency regions. By the numerical experiments, we find that the classical crossover corresponds to a chaotic orbit in phase space as in Fig. 3(a). However, in other frequency regions, the classical dynamics are regular and the classical trajectories are located in the initially occupied well as in Figs. 3(b) and 3(c). By decreasing the driving amplitude

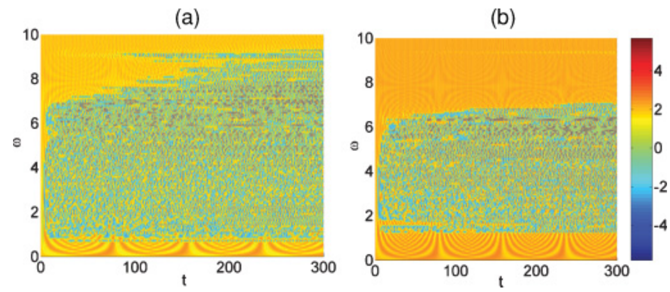

FIG. 2. (Color online) Time evolution of the classical trajectories $x(t)$ for different driving frequencies. The parameters are chosen as $a = 5$, $b = 0.25$, and (a) $\varepsilon = 3$, (b) $\varepsilon = 2$. Initial position and momentum of the particle are set as $x_0 = \sqrt{5}$ and $p_0 = 0$, respectively.

to $\varepsilon = 2$, the moderate-frequency region becomes small as in Fig. 2(b), which indicates that the range of the driving-frequency region depends on the driving amplitude. In this paper, we focus on the quantum tunneling behaviors of single particles for the three different driving-frequency regions.

A. Chaotic behavior in the moderate-frequency region

First, we consider the quantum dynamics of a single particle in the moderate-frequency region, where the classical dynamics governed by Eq. (3) may be chaotic [8]. The initial state is set as the Gaussian wave packet [16]

$$\Psi(x,t=0) = (\sigma\pi)^{1/4} \exp\left[-\frac{(x-x_0)^2}{2\sigma}\right], \tag{4}$$

with the center position $x_0 = \sqrt{5}$ and expectation value of momentum $\bar{p}_0 = 0$; the spread of the initial packet is taken as $\sigma = 0.3$. The boundary conditions $\Psi(x = \pm\infty,t) = 0$ are satisfied in the numerical calculations. Numerically, we find the irregular quantum tunneling for the moderate-frequency driving, as in Fig. 4, where spatiotemporal evolution of the probability density $|\Psi(x,t)|^2$ is exhibited for the same driving parameters as in Fig. 3(a). The distribution of probability density is irregular and at any time it fills the two wells centered at $x > 0$ and $x < 0$, respectively. It exhibits a high tunneling rate, an important characteristic of the chaos-assisted tunneling [16].

B. CDT in the sense of the time average in the low-frequency region

Now we investigate the quantum dynamics for low-frequency driving from Eq. (1), where the classical trajectory

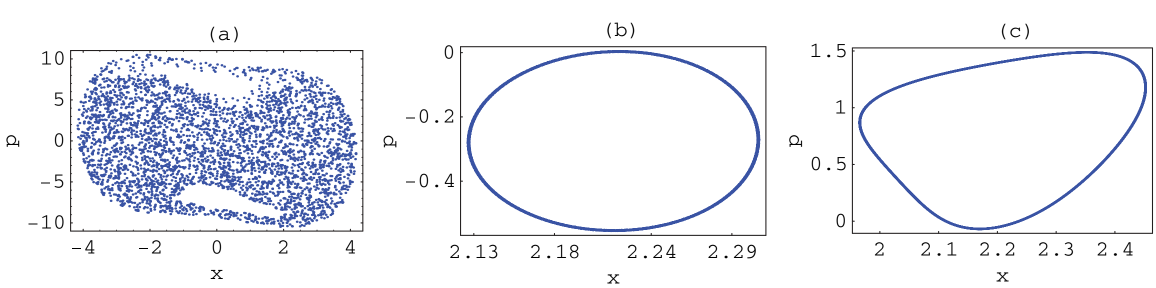

FIG. 3. (Color online) Stroboscopic plots of the classical trajectories in phase space for the driving parameters $\varepsilon = 3$ and (a) moderate frequency, $\omega = 2.5$; (b) low frequency, $\omega = 0.45$; and (c) high frequency, $\omega = 9.6$. The initial conditions are the same as those in Fig. 2.

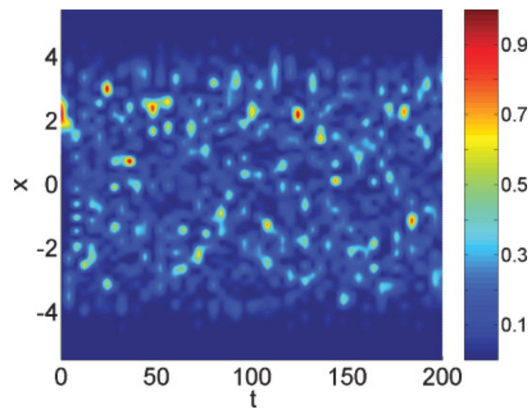

FIG. 4. (Color online) Spatiotemporal evolution of the probability density with parameters $\varepsilon = 3$, $\omega = 2.5$, and initial state of Eq. (4).

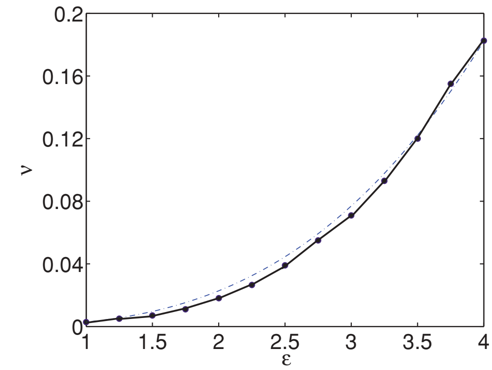

FIG. 6. (Color online) Numerical result of parameter ν vs driving strength ε (black dots) and the function $\nu(\varepsilon) = 0.002\,85\varepsilon^3$ (dash-dotted line).

located in the initially occupied well is regular, as illustrated in Fig. 3(b) for $\varepsilon = 3$, $\omega = 0.45$ ($\omega < 0.5$). For the same driving amplitude $\varepsilon = 3$, a set of resonance-like frequencies, $\omega_n = \nu/n$ with constant $\nu = 0.0708$ and $n = 1,2,\ldots,$ is found by numerical methods. Periodic spatiotemporal evolution of the probability density is exhibited for the driving frequency $\omega_1 = 0.0708$ as in Fig. 5(a), where the quantum tunneling of the probability density wave packet occurs around the lowest barrier at $t = t_k(\omega_1)$. In a short time interval δt, the wave packet tunnels through the lowest barrier and rapidly returns to the initially occupied well; then it is located in the initial well for a long interval $\Delta t_k(\omega_1) = t_{k+1} - t_k - \delta t \approx 77$ with $\delta t \approx 7 = \Delta t_k(\omega_1)/11$ being the time located in the other well. Such a process is repeated periodically. So the quantum probability in the right well reads $P_R(t) = \int_0^\infty |\Psi(x,t)|^2 dx = 1$, except for the short time δt.

Keeping the strength $\varepsilon = 3$ and decreasing the driving frequency to $\omega_2 = \nu/2 = 0.0354$, the spatiotemporal evolution of the probability density is illustrated in Fig. 5(b). It is shown that the probability density wave packet returns to the initially occupied well after four tunneling events around the lowest barrier, where the wave packet is located completely in the initial well in the time interval $\Delta t_k(\omega_2) = t_{k+1} - t_k + \delta t - 2\delta t \approx 11 \times 2\delta t = 154$ and the time in the other well is approximately $2\delta t$ during one time period. In Figs. 5(c) and 5(d), similar results are found for $\omega_3 = \nu/3$ and $\omega_4 = \nu/4$. In fact, for any $\omega_n = \nu/n$ with $n = 1,2,\ldots,$ we have obtained $\Delta t_k(\omega_n)/(n\delta t) \approx \Delta t_k(\omega_1)/\delta t \approx 11$; that is, the time located in the initially occupied well $\Delta t_k(\omega_n)$ is 11 times that of the time in the other well, $n\delta t$. This implies the interval $\Delta t_k(\omega_n) = n\Delta t_k(\omega_1)$, which increases with increasing n. The result reveals that the particle is always located in the initially occupied well except for a short time $n\delta t$ for driving frequency ω_n. So the time-averaged probability is $\overline{P}_R = \frac{1}{mT}\int_0^{mT} P_R(t)\,dt \approx 0.92$, with m an integer, which reveals the approximate CDT in the sense of the time average. Of course, the CDT in the sense of the time average is different from that reported by Grossmann *et al.* [9], which can be well understood by a two-state model in the high-frequency approximation [7]. However, the CDT presented here is obtained in the low-frequency region by solving the exact Schrödinger equation (1) instead of the approximate two-state model. Interestingly, the CDT in the sense of the time average is similar to the strong self-trapping phenomenon, which has been realized in an experiment based on Bose-Einstein condensates [1].

When the driving strength ε is changed, we find that the parameters ν and ω_n depend on ε. In Fig. 6, we show the parameter ν versus the driving strength ε numerically by the black dots and the approximate functional relation between ν and ε, $\nu(\varepsilon) = 0.002\,85\varepsilon^3$, by the dash-dotted line. To our surprise, the relation of the discrete driving-frequency $\omega_n = \nu/n$ is similar to the condition of multiple photon resonance [12–14], where $\omega_n = \Delta E/n$ with ΔE the potential difference of two adjacent wells. It is well known that the multiple photon resonance can cause CDT to depend on the quantum number n [12–14]. However, for the driving frequency $\omega \neq \nu/n$, the particle possesses an approximately equivalent time-average

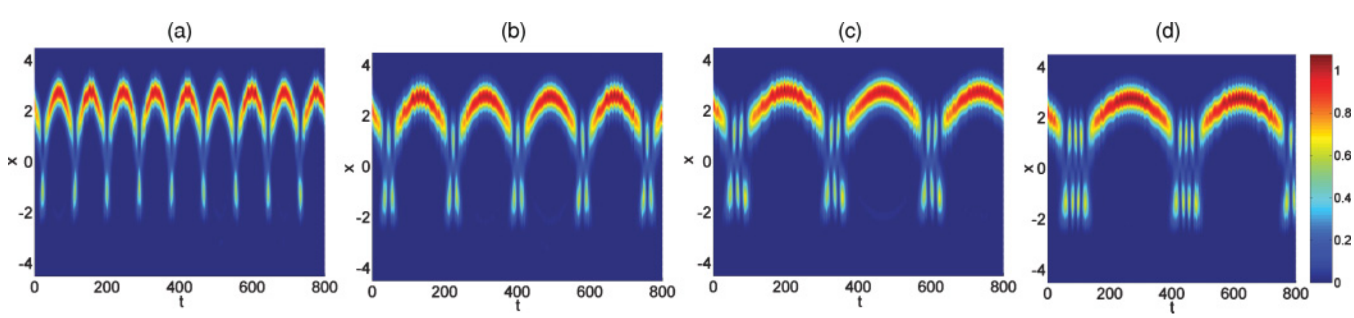

FIG. 5. (Color online) Spatiotemporal evolution of the probability density for the driving strength $\varepsilon = 3$ and frequencies $\omega_n = 0.0708/n$ with (a) $n = 1$, (b) $n = 2$, (c) $n = 3$, and (d) $n = 4$. The initial state is given by Eq. (4).

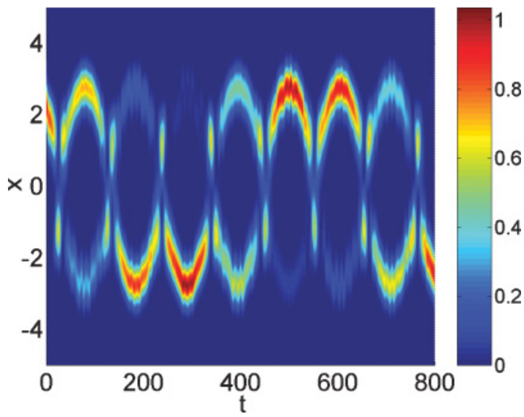

FIG. 7. (Color online) Spatiotemporal evolution of the probability density for $\varepsilon = 3$, $\omega = 0.059$.

value of probability in the two wells, as shown in Fig. 7, where the quantum probability obeys $\overline{P}_R \approx \overline{P}_L \approx 0.5$. So, the CDT in the sense of the time average can be obtained only for the discrete resonance-like frequency ω_n in the low-frequency region. This result is very interesting and may be important for the design of a single-particle device [18].

C. Long-lasting localization in the high-frequency region

When a particle is located at the bottom of one well for a long time, we could call the phenomenon long-lasting localization, compared to similar behavior in the recent experiment with a light coupler [15]. For the high-frequency case, we demonstrate such a long-lasting localization in this subsection. Usually, the high-frequency field varies so rapidly that the wave function is not able to respond appreciably and thus remains nearly constant over one period [19]. This assumption is suggested by exploring the behavior of the high-frequency driven harmonic oscillator [20], where the transformation $\Psi(x,t) = \Phi(x,t)e^{i\frac{\varepsilon}{2\omega}x^2\cos(\omega t)}$ with $\Phi(x,t)$, a slowly varying function of time, is adopted. Correspondingly, the probability density becomes $\rho(x,t) = |\Psi(x,t)|^2 = |\Phi(x,t)|^2$, and the time-dependent driving field $\mu(x,t) = \frac{\varepsilon}{2}x^2\sin(\omega t)$ is replaced by the time-independent effective potential $\mu_{\rm eff} = \frac{\varepsilon^2}{4\omega^2}x^2$ in the high-frequency approximation [19]. This means that the physical effect on the tunneling dynamics of the particle is related to the ratio ε/ω for a high enough driving frequency ω.

Let us now numerically investigate the long-lasting localization from Eq. (1) with high driving frequency, where the classical trajectory is regularly located in the initially occupied well. Spatiotemporal evolution of the probability density wave packet is exhibited for $\varepsilon/\omega = 0.32$ as in Fig. 8(a), where the wave packet stays at the bottom of the initially occupied well in the half-period $\tau(\varepsilon/\omega)/2$, with $\tau(0.32) \approx 330$ being the evolution period in time, and then rapidly tunnels to the other well. Clearly, the wave packet is located at the bottom of each well alternately and the evolution period τ is much longer than the driving period $T = 2\pi/\omega$ for any driving frequency in the high-frequency region $\omega > 8.9$. In Figs. 8(b), 8(c), and 8(d), we display the spatiotemporal evolutions of the probability density wave packet for the lower ratios $\varepsilon/\omega = 0.28$, 0.2, and 0.1, respectively. It is shown that the time located in each well, $\tau(\varepsilon/\omega)/2$, rapidly increases with the decrease of the ratio ε/ω. When $\varepsilon/\omega = 0.1$ is considered, the time $\tau(0.1)/2$ exceeds 1500, which indicates that the particle stays in the initially occupied well for quite a long time. A similar experimental phenomenon was observed recently for light couplers [15].

III. SUMMARY AND DISCUSSION

In summary, we have investigated the tunneling dynamics of a single particle initially located in one of the driven double wells with zero momentum. Three frequency regions are given based on Newton's classical equation. In the moderate-frequency region, it is demonstrated that the classical dynamics is chaotic and the quantum tunneling is irregular. For other frequency regions, the classical dynamics are regular and corresponding tunneling behaviors exhibit some interesting features. In the low-frequency region, the spatiotemporal evolutions of probability density show that the particle is always located in an initially occupied well, except for n oscillations around the lowest barrier for a set of discrete driving frequencies ω_n, and the time evolution of probability density exhibits the approximate CDT in the sense of the time average. Such a resonance-like phenomenon is similar to multiple photon resonance [12–14]. In the high-frequency region, the long-lasting localization alternately in each well is demonstrated and the time located in one well increases with the decrease of the ratio ε/ω. This is similar to the recently reported result on light evolution in dynamically modulated directional couplers [15]. The results presented in this paper can be easily verified under presently accessible experimental conditions for controlling single-atom tunneling [11].

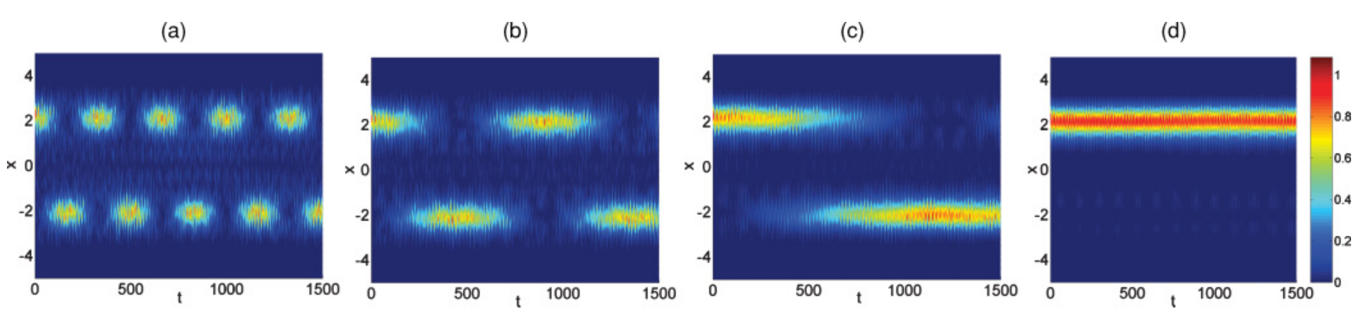

FIG. 8. (Color online) Spatiotemporal evolution of the probability density for different driving parameters: (a) $\varepsilon/\omega = 0.32$, (b) $\varepsilon/\omega = 0.28$, (c) $\varepsilon/\omega = 0.2$, and (d) $\varepsilon/\omega = 0.1$. The initial state is given by Eq. (4).

ACKNOWLEDGMENTS

The authors thank Xiaobing Luo for helpful discussions of the numerical work. This work was supported by the National Natural Science Foundation of China under Grant No. 10875039, the Construct Program of the National Key Discipline, the PCSIRT under Grant No. IRT0964, and the SRFDPHE.

[1] M. Albiez, R. Gati, J. Fölling, S. Hunsmann, M. Cristiani, and M. K. Oberthaler, Phys. Rev. Lett. **95**, 010402 (2005); Q. Xie and W. Hai, Phys. Rev. A **75**, 015603 (2007); X. Luo, Q. Xie, and B. Wu, *ibid.* **77**, 053601 (2008).

[2] J. Javanainen, Phys. Rev. Lett. **57**, 3164 (1986); M. W. Jack, M. J. Collett, and D. F. Walls, Phys. Rev. A **54**, R4625 (1996); G. Ferrini, A. Minguzzi, and F. W. J. Hekking, *ibid.* **80**, 043628 (2009).

[3] A. Eckardt, T. Jinasundera, C. Weiss, and M. Holthaus, Phys. Rev. Lett. **95**, 200401 (2005); N. Teichmann, M. Esmann, and C. Weiss, Phys. Rev. A **79**, 063620 (2009).

[4] M. Grifoni and P. Hänggi, Phys. Rep. **304**, 229 (1998).

[5] A. Sethi and S. Keshavamurthy, J. Chem. Phys. **128**, 164117 (2008).

[6] H. Fielding, M. Shapiro, and T. Baumert, J. Phys. B: At. Mol. Opt. Phys. **41**, 070201 (2008).

[7] G. Lu, W. Hai, and H. Zhong, Phys. Rev. A **80**, 013411 (2009).

[8] W. A. Lin and L. E. Ballentine, Phys. Rev. Lett. **65**, 2927 (1990); G. M. D'Ariano, L. R. Evangelista, and M. Saraceno, Phys. Rev. A **45**, 3646 (1992).

[9] F. Grossmann, T. Dittrich, P. Jung, and P. Hänggi, Phys. Rev. Lett. **67**, 516 (1991); Z. Phys. B **84**, 315 (1991); G. Grossmann, and P. Hänggi, Europhys. Lett. **18**, 571 (1992).

[10] P. S. S. Guimaräes, B. J. Keay, J. P. Kaminski, S. J. Allen Jr., P. F. Hopkins, A. C. Gossard, L. T. Florez, and J. P. Harbison, Phys. Rev. Lett. **70**, 3792 (1993); B. G. Bale, S. Boscolo, J. N. Kutz, and S. K. Turitsyn, Phys. Rev. A **81**, 033828 (2010).

[11] E. Kierig, U. Schnorrberger, A. Schietinger, J. Tomkovic, and M. K. Oberthaler, Phys. Rev. Lett. **100**, 190405 (2008).

[12] C. Sias, H. Lignier, Y. P. Singh, A. Zenesini, D. Ciampini, O. Morsch, and E. Arimondo, Phys. Rev. Lett. **100**, 040404 (2008).

[13] M. Holthaus, G. H. Ristow, and D. W. Hone, Phys. Rev. Lett. **75**, 3914 (1995).

[14] C. E. Creffield and T. S. Monteiro, Phys. Rev. Lett. **96**, 210403 (2006).

[15] A. Szameit *et al.*, Opt. Lett. **34**, 2700 (2009).

[16] A. Igarashi and H. Yamada, Chem. Phys. **309**, 95 (2005); **327**, 395 (2006); Phys. Rev. E **78**, 026213 (2008).

[17] T. Jinasundera, C. Weiss, and M. Holthaus, Chem. Phys. **322**, 118 (2006).

[18] Z. Kim, V. Zaretskey, Y. Yoon, J. F. Schneiderman, M. D. Shaw, P. M. Echternach, F. C. Wellstood, and B. S. Palmer, Phys. Rev. B **78**, 144506 (2008).

[19] R. J. Cook, D. G. Shankland, and A. L. Wells, Phys. Rev. A **31**, 564 (1985).

[20] K. Husimi, Prog. Theor. Phys. **9**, 381 (1953); E. H. Kerner, Can. J. Phys. **36**, 371 (1958).